

Stellar disks and halos of the edge-on spiral galaxies: NGC 891, NGC 4144 and NGC 4244

Tikhonov N.A. and Galazutdinova O.A.

Special astrophysical observatory RAS

Abstract

The results of the stellar photometry of the images ACS/WFC and WFPC2 of the HST are used to study stellar population and spatial distribution of stars in three edge-on galaxies: NGC 891, NGC 4144 and NGC 4244. The measuring of the number density of the old stars revealed two stellar substructures in these galaxies: thick disk and halo. The borders of these substructures consisting mainly of red giants, are determined by the change of number density gradient of the old stars. The revealed halos have flattened shapes and extend up to 25 kpc from the galaxy planes. The obtained results of number density distributions of different type stars perpendicular to the galaxy planes allow us to verify our stellar model of spiral galaxies. Using the determination of the tip of red giant branch (TRGB method) we have derived the following distances: $D = 9.82$ Mpc (NGC 891), $D = 7.24$ Mpc (NGC 4144) $D = 4.29$ Mpc (NGC 4244).

1 Introduction

By the present time the stellar population of galaxies has been studied in sufficient details only in the nearest stellar systems of the Local group where three spiral galaxies: M 31, M 33 and Galaxy dominate. In the named of spiral galaxies four stellar subsystems are generally distinguished: a bulge, a thin disk, a thick disk and a halo. These subsystems have different laws of spatial distributions of stars and consist of stars and clusters with a different average age and the mean metallicity value [1–6]. Due to the fact that these subsystems are embeded one into another, it is difficult to define the space boundaries of these subsystems since the inner subsystem also contain stars of the outer subsystems. The division of stars into subsystems is usually performed on the basis of measurements of photometric parameters of stars,

their metallicity value and kinematic characteristics. The technical difficulties at the vast determinations of characteristics of stars and the uncertainty in the terminology when describing stellar morphology of galaxies cause some chaos in the designation of the studied stellar structures of galaxies. The circumstance that observations of galaxies are carried out in different spectral bands, which naturally leads to changes in the visible morphology of galaxies, makes the chaos worse. On the basis of surface photometry methods the procedure of division of spiral galaxies into two components: a bulge and disk [7] has been developed reliably enough. By the term “disk”, a thin disk, where star formation is currently in progress, and the bright part of a thick disk inhabits by older stars is implied. As far as a stellar halo of galaxies is concerned neither the shape of the halo nor the law of the decrease of number density toward the outer part of the halo are known yet.

By analogy with spiral galaxies of the Local group search for thick disks and halos are being carried out in more distant galaxies. For instance, on the basis of studying of 47 late types galaxies it has been found that most of these galaxies possesses a thick disk [8]. However, this is more likely to be a qualitative pattern of the structure of galaxies. Since for revealing thick disks methods of surface photometry were used, the determination of age composition of stellar disks and establishment of their borders are extremely involved problems. The situation with the search for and determination of halos turns out to be even more intricate. In a number of papers the term “halo” is used to name any stellar structure beyond the border of thin disk. In this case the term “thick disk” is absent and its place is taken by the term “halo”. Naturally, such a pseudo-halo can be recorded in some galaxies by the methods of deep surface photometry. For the theories of origin and evolution of galaxies it is extremely necessary to have uniform and reliable results on extended stellar structures of galaxies since they mostly consist of old stars with low metallicity and keep information about the first stages of evolution of galaxies. Many results on stellar composition of nearby galaxies have already been obtained, but the main step should be made and define the conception disks and halos. Without such definitions continuous confusion will take place in designations of those stellar structures which are observed in galaxies with using various techniques. Irregular galaxies, which are the close relatives of spiral galaxies, have the simplest composition. The discovery of a stellar halo in two irregular galaxies, WLM and NGC 3109, was announced in the papers by Minniti and his colleagues [9], [10]. Later, based on the study of the stellar population of 25 irregular galaxies, Tikhonov [11-13] showed

that every irregular galaxy has a thick disk the dimensions of which are 2–3 times as large as the visible body of the galaxy. Young stars in irregular galaxies concentrate toward the galactic plane and form a disk similar to thin disks of spiral galaxies. The study of massive irregular galaxies has shown that besides a thick disk they may also have a halo that extends to a distance greater than the thick disk and has a different gradient of decrease in stellar number density. By the present time, we have found such halos around a few massive irregular galaxies: IC 10, M 82, NGC 3077. On the basis of these results it becomes clear that Minniti and his colleagues are likely to have found in the galaxies WLM and NGC 3109 thick disks, but not halos, since they have not found bend of the density gradient of red giants and the sharp drop of stellar density at the border of the thick disk as it is seen in the galaxy IC 10 [14], [11] and M 82. Three spiral galaxies, NGC 55, NGC 300 and M 81, that we investigated earlier show the presence of a thick disks and a halos [15] which unites its morphologically with massive irregular galaxies. In order to understand the spatial structures of thick disks and halos, it is necessary to investigate edge-on galaxies since only with such position of galaxies we can see and study the extent of the thick disk and halo perpendicular to the galactic plane. In the present paper we fill the existing gap and present the results of investigation of the stellar population of three edge-on galaxies. The basic characteristics of these galaxies are listed in Table 1. All the galaxies have a developed spiral structure, and their luminosity is comparable with the luminosity of our Galaxy.

1.1 NGC 891

. The galaxy NGC 891 belonging to the NGC 1023 group is morphologically the most identical to our Galaxy. It might be expected that it also has similar physical conditions, however, the current rate of star formation in NGC 891 is 2–3 times as high as that in our Galaxy.

The age of NGC 891 is estimated to be 11–13 billion years [16], [17], which within the errors, corresponds to the age of our Galaxy equal to 13.6 billion years [18]. NGC 891 has been intensively studied in all spectral bands. The investigation of optical images (BVI+H α) of NGC 891 shows two physically different components of the interstellar disk of this galaxy: dense cold one visible on BVI images in the form of absorption and consisting of structured dust clouds traced to 2 kpc from the galactic plane and a warm ionized one, visible on H α images and uniformly distributed over the body

of the galaxy with inclusion of thread-like structures [19]. Photographic observations of NGC 891 on red and blue plates has revealed two stellar components — a bulge and a disk [20], the border of the disk was traced almost to the border of the thick disk that we have found on the basis of searching of stellar number density. Radio investigations of NGC891 have shown that the galaxy has a gaseous halo, where one observed CO [21] and atomic hydrogen [22], extending to 5 kpc from the galactic plane and being of $\sim 15\%$ of the total mass of neutral hydrogen. The most remote HI clouds have been recorded to a distance of up to 15 kpc from the galactic plane [23],[24]. The diameter of the hydrogen disk of NGC 891 is 1.2 times as large as the optical diameter of the galaxy determined from the level of the isophote $\mu = 25^m/\text{sq.arcsec}$ in the B band [25]. When using a axially-symmetrical model of the distribution of stars and dust, three parameters were determined for NGC 891, which describe best the distribution of stars and dust in the optical and IR regions [26]. The scale height in this model is equal 0.4 kpc for the stars and 0.26 kpc for the dust. The model gives the mass of dust $1.14 \times 10^8 M_{\odot}$ and $M_{gas}/M_{dust}=1.65$, which is close to the value obtained for our Galaxy [27].

1.2 NGC 4144

Due to its high distance and absence of any morphology peculiarities, the galaxy NGC 4144 becomes most frequency as an object of statistical investigations of galaxies only [28-30]. A comparison of HI radio observation and optical observations in the B and R bands has shown that the galaxy possesses a thick hydrogen disk whose dimensions exceed those of the visual body of the galaxy [31], [32].

2 NGC 4244

The galaxy has a low of star formation rate and is surprisingly quiet in the radio continuum [33]. Observations of atomic hydrogen show that on the Z axis hydrogen is seen up to a height of $2.5'$ (3.1 kpc) [34]. The diameter of the hydrogen disk is 1.3 times larger than the optical diameter at $\mu = 25^m/\text{sq.arcsec}$ in the B band [25]. The galaxy is of low luminosity in the filter $H\alpha$ and of low surface brightness in the far IR [35]. The deep CCD photometry (up to 27.5 stellar magnitudes in the R band) shows that NGC 4244

has a simple structure: an exponential disk with a scale height of 250 pc. No evidence of existence of the second component, a thick disk or a halo, has been found [36].

3 Observations

To study the stellar population of the galaxies, we used the archive images obtained in different years with the ACS/WFC and WFPC2 of the Hubble Space Telescope (HST). The information about the archive images that we have used is in Table 2.

Figs.1, 2 and 3 present the DSS images of the investigated galaxies with ACS/WFC and WFPC2 footprint overlaid. The stellar photometry was performed with the packages of programs DAOPHOT II in MIDAS and HST-PHOT [37], [38]. The reduction of DAOPHOT instrumental stellar magnitudes to the standard Kron-Cousins system was executed by the procedure described in the papers by Holtzmann et al. [39],[40]. The reduction of the ACS/WFC results to the standard VI system was performed on the basis of calibration relationships for the stars in the galaxy IC 10 where we fulfilled photometry of the same stars as both in ACS/WFC and in the WFPC2 frames. To obtain colour relationship 60 calibration stars with $0 < (V - I) < 5$ were employed. The accuracy of the reduction of stellar magnitudes is equal to 0.03^m for the I band and 0.04^m for the V ones.

The derived equations of the reduction of instrumental stellar magnitudes into the VI Kron-Cousins system were checked by us at the stars of the known galaxies (NGC 55, NGC 300) and showed a good agreement of the obtained results with the results of other authors. Background distant galaxies, unresolved stars due to superposition of images of close neighbors and stars ruined because of the defects of the CCD chips were excluded from the final list on the basis of comparison of their profiles with the standard star PSF profile. The stars that were left in the final lists had the following parameters: “SHARP” < 0.3 , and “CHI” < 1.2 [37].

4 Selection of stars

To ensure maximum homogeneity of the sample of stars of different fields, we made selection of stars basing on the following conditions: a) To exclude

the effect the duration of the exposure has on the number of stars found in the field (images of different research programs were used for different fields) we used the results obtained with the shortest exposure. For all the studied fields of one galaxy we set the same border in luminosity of stars. Stars more fainter were not used even if they were seen in the images of some fields of the galaxy. b) The process of filtering of traces of cosmic particles removed them to a considerable degree, and the particle could not distort the counts of stars number density in crowded stellar fields. However, in sparse stellar fields the number of unremoved traces of cosmic particles (i.e. fictitious stars) is comparable with the number of real faint stars. This effect leads to an imaginary decrease in the gradients of star number density in the searching fields. In order to eliminate this effect, we had to use stars by 0.5^m stellar magnitude brighter than the photometric limit of the images since the program of filtering particles is unable to remove the faintest traces of particles. Such constraints reduced the number of stars in the fields and increased statistical noise, but to make up for it, we could be certain that our results of measuring the number density of stars are not affected by the residual traces of cosmic particles.

5 Results of photometry

5.1 “Colour–magnitude” diagrams of the galaxies: NGC 891, NGC 4144, NGC 4244.

The results of stellar photometry are presented in Fig.4 in the form of “Colour – Magnitude” diagrams (CMD). The obtained diagrams are typical of spiral galaxies. The considerable differences in the diagrams of different fields of one and the same galaxy can readily be explained since the fields under investigation may cover both the regions of spiral arms with bright supergiants and the regions of halos where AGB stars can be the brightest stars, but the main population visible in the images is the red giants. Lines are drawn on all the diagrams, which show the position of the tip of the red giant branch (TRGB) used for measurement of distances. In the field S2 of the galaxy NGC 891, which is the most poorly populated by stars, only the tip of the red giant branch is visible at $(V-I) = 1.5$ and a comparable number of background stars. Due to the closeness of the photometric limit of the images of this field to the luminosity of the searching stars, we moderated our

criteria of selection of red giants for this unique case, following from the real assumption of large photometric errors of these faint stars. Our criteria for this field are: $1.0 < (V - I) < 2.2, I > 25.7$.

5.2 Measurement of distances

The presence of stars of the red giant branch on the “Colour–Magnitude” diagrams that we derived (Fig.4) enables to measure accurate distances to the galaxies by using the TRGB method [41].

To calculate the distances, we used one or two fields in each galaxy, avoiding star formation regions with bright supergiants and choosing regions containing a great number of red giants in order to diminish the statistical error in the determination of the tip of red giant branch. We used the fields S2 in NGC 891 (Fig.1), S1 in NGC 4144 (Fig.2), S1, S2 and S3 in NGC 4244 (Fig.3).

The luminosity function in the I band of stars in each field has a jump which corresponds to the beginning of the red giant branch (Fig.5). Given the apparent stellar magnitude of the tip of red giants branch, one can measure the distance to the galaxy by the TRGB technique [41]. Simultaneously with the determination of the distance the average metallicity of red giants in the region of the galaxy being investigated was measured.

It should be noted that due to the gradients of metallicity of red giants along the radius of the galaxy, the local metallicity values that we obtained cannot be regarded to be the metallicity of red giants of the whole galaxy and use them for construction of global statistical relationships of parameters of galaxies. This remark does not refer to dwarf irregular galaxies where the gradient of metallicity along the radius of a galaxy is likely to be very insignificant. Using the red giants of the ACS/WFC image beyond the border of the thick disk of NGC 891 (Fig.1), we derived the value of $I_{TRGB} = 25.97$, which corresponds to $(m - M) = 29.96 \pm 0.08$, $D = 9.82 \pm 0.37$ Mpc) at $[\text{Fe}/\text{H}] = -0.74$. The red giants of this galaxy have the highest metallicity of all three galaxies. This is defined by the fact that the galaxy NGC 891 also has the greatest mass preventing the outflow of metals outside the border of the galaxy. The measurements of the distance to NGC 891 were made earlier on the basis of the luminosity function of planetary nebulae and the method of the surface brightness fluctuations[42]. The mean distance module obtained by these methods is $(m - M) = 29.95 \pm 0.10$, which corresponds to $D = 9.77$ Mpc. The discrepancy with our results is very insignificant.

In the ACS/WFC field of the galaxy NGC 4144 we used red giants of thick disk and halo outside the border of the main body of the galaxy. The tip of the red giant branch is well noticeable at $I_{TRGB} = 25.20$, which corresponds to the distance modulus $(m - M) = 29.30 \pm 0.10$ ($D = 7.24 \pm 0.35$ Mpc) at the mean metallicity of red giants $[\text{Fe}/\text{H}] = -0.82$. The distance to this galaxy, $D = 9.7$ Mpc was obtained earlier on the basis of photometry of the brightest supergiants [43]. The difference between this result and our value can be explained by the inclination of the galaxy, when only part of the galaxy is visible and the calibration relations between the total luminosity of the galaxy and the luminosity of the brightest stars may have a great error.

For NGC 4244 we obtained $I_{TRGB} = 24.14$ and $[\text{Fe}/\text{H}] = -1.62$ for S1, $I_{TRGB} = 24.20$ and $[\text{Fe}/\text{H}] = -1.66$ for S2 and $I_{TRGB} = 24.15$ and $[\text{Fe}/\text{H}] = -0.85$ for S3. The average distance modulus is $(m - M) = 28.16 \pm 0.08$, which corresponds to ($D = 4.33 \pm 0.16$ Mpc). The discrepancies in the obtained metallicity values are due to the fact that when calculating TRGB and the metallicity of the red giants in S1 and S2 fields, we used stars at a maximum distance from the galactic plane, where a low-metallicity population is observed and bright AGB stars are absent. This improved the accuracy of measuring the distance to the galaxy, and in the S3 field stars were selected within the thick disk. The distance that we measured is consistent, within the errors, with the distance $D = 4.49$ Mpc obtained by Karachentsev et al. [44] on the basis of photometry of the red giants of the field S1.

5.3 Distribution of stars over the body of galaxies

The three galaxies being investigated are viewed nearby exactly edge-on, and we could study of the number densities of different type stars perpendicularly to the equatorial plane of the galaxy (Figs.6, 7, 8). The principal difficulty we had to overcome when preparing the results was the scatter and discontinuity of the fields of observations which we used to study the spatial distribution of stars. When interpolating the results of the number density of stars of different subsystems, we proceeded from the assumption that thick disks and halos are of smooth, axially symmetric shape, without any tidal distortions. It can be seen from Figs. 7 and 8 that the chaotic fluctuations of stellar density near the equatorial plane of the galaxy disappear with increasing distance from the plane of the galaxy, and the relationship “number density - Z coordinate” assume an exponential form. This is explained by the fact that at small distances from the equatorial plane screening of stars by gaseous-

dust matter of the galaxy decreases essentially the luminosity of stars, and faint stars cease to be visible. Besides, excess number density of stars is observed near the equatorial plane. Under these conditions the automated program FIND of DAOPHOT II terminated recognition of closely spaced stars and does not include them in the list of photometry.

The two causes mentioned lead to a fictitious decrease in the computed star number density, which we observe in Figs.7 and 8 at small distances from the galactic plane. For the regions remote from galactic plane, the exponential change of the stellar density, with no distorting factors being present, points to a disk's character of stellar subsystems [45].

5.3.1 NGC 891

As can be seen from Fig.1 the areas that we used are located along the minor axis of the galaxy. The orientation of the image of the ACS camera is not quite convenient for calculations of the star number density along the Z axis, but in return it allows the variation of this density to be traced a great distance. The region of the image near the galactic plane have considerable deficiency of red giants due to the effects of screening the opposite parts of the disk and halo by the body of the galaxy, therefore we observe a dip of number density of red giants there. Similar but a smaller dip of density is observed for brighter AGB stars as well. We excluded these regions absorption from the plot the distribution of the number density of stars along the Z axis to visualize better the behavior of the number density of AGB and RGB stars at the boundary of the thick disk and halo (Fig.6). The behavior of the number density of stars of different types near the galactic's plane will be discussed in more detail below by the examples of the galaxies NGC 4144 and NGC 4244 (Figs. 7 and 8).

The boundary of the thin disk in spiral galaxies is defined by the region of spread of gaseous-dust clouds and young stars. In NGC 891 this boundary is outside the interval in the Z coordinate, which is presented on the diagram in Fig.6. That is all AGB and RGB stars the distribution of which is shown in Fig.6 belong to the thick disk and halo. AGB stars in the disk of NGC 891 display a sharp drop in number along the Z coordinate, and outside the limits $Z = 6$ kpc (Fig.6a) their number is small. The number of RGB stars decrease essentially slower, and the point change of the gradient of their member density, that is the boundary of the thick disks becomes noticeable (Fig.6b). Probably, the matter is that massive galaxies viewed edge-on have

a halo with a large stellar density gradient of comparable with that of stellar density of the thick disk, and the revealing of the bend point of the number density of stars in such galaxies is an involved problem. The bend of the density gradient in RGB stars is observed at $Z = 7.6$ kpc (Fig.6b). By analogy with the results for face-on galaxies [15] the bend point of the density of red giants defines the boundary of the thick disk and the beginning of the more extended halo. Having calculated the density gradient of RGB stars from the inner part of the halo, we extrapolated the changes of stellar density to zero values of the number density of stars. Thus, we computed that the supposed size of the halo along the Z axis is equal to 26.9 Kpc. We chose the exponential character of the drop in the density of halo stars by analogy with the thick disk. Fortunately, the field WFPC2 (S2) was found exactly at the supposed boundary of the halo, which confirmed the legitimacy of our extrapolation and permitted to refined the size of the halo. Fig.6c shows the behavior of the number density of RGB stars in the field S2. The stellar density diminishes along the Z axis and falls to the background values at $Z = 23$ kpc, which nearby coincides with the result of our extrapolation as to the size of the halo. Thus, the measurements show that NGC 891 has a thick disk of 15 kpc in thickness and a halo with a size of 46 kpc, along the Z coordinate. Proceeding from the assumption that the gradient of the decreasing of stellar density along the major axis has the same value (generally, it has smaller value) as along the minor axis, it follows from thus assumption that the halo is oblate at the poles of the galaxy. It is seen in Fig.1 that assuming the found boundaries of the halo as a basis, we cannot inscribe the round spherical halo into the dimensions of the galaxy, that is, the halo of NGC 891 is an oblate ellipsoid in shape. Such a shape is not unexpected since the oblateness of the halo at the poles is likely to be also observed in the galaxy M 31 by the visible surface distribution of bright red giants [46].

5.3.2 NGC 4144

Fig.7 displays the plots of the number density distribution of young stars, stars of intermediate age (AGB) and old stars (RGB). The young stars in the ACS/WFC image are distributed on the outer side of the thin disk at a certain optical depth, which is evidenced by the broadening of branch of blue supergiants (Fig.4). These stars has a maximum visual brightness and are slightly affected by the brightness and inhomogeneity of the background

near the galaxy plane. This can be seen on the diagram of Fig.7, where the decrease of their number density in the distribution of stars is not noticeable. Intermediate age stars (AGB) have a smaller gradient of number density, as compared to young stars have, and extend to larger distances from the galactic plane than young stars. The most numerous stars — red giants have the smallest gradient of the number density. At distances $Z = 2.4$ kpc from the galactic plane, NGC 4144 shows a change of the number density gradient of RGB stars as in the galaxy NGC 891. We assume this point to be the boundary of the thick disk. At larger distance from the galactic plane, in the halo region, extrapolation of the exponential decreasing of the number density of stars makes it possible to compute the boundary of the halo ($Z = 5.4$ kpc). The same as for the galaxy NGC 891, the halo of NGC 4144 has an oblate shape at the poles of the galaxy.

5.3.3 NGC 4244

Although the galaxy NGC 4244 resembles NGC 4144 both in morphology and stellar composition, there are some differences of its parameters of outer stellar structures. Fig.8 shows plots of the number density distribution of stars of different age. The same as in NGC 4144, young stars of NGC 4244 concentrate in the most narrow equatorial region. Intermediate age stars have a wider distribution, while old stars have a minimum gradient of the number density and occupy the most extended region. The difference between the galaxies is that the plot (Fig.8a) shows no bend point of the number density of red giants in NGC 4244, which would correspond to the boundary between the thick disk and the halo. To clear up the point whether a halo exist or not in this galaxy we have studied the distribution of red giants in the fields S1 and S2 of the WFPC2 (Fig.3). The field S1 does not fall outside the thick disk of the NGC 4244 and no changes in the density gradient are noticeable in the number density distribution of red giants (Fig.8). However, in the field S2 the distribution of RGB stars shows a sharp change of the number density of stars along the Z axes. To the $Z = 2.7$ kpc the number density gradient corresponds to that of the field ACS/WFC, but at greater distances from the galactic plane the number density gradient undergoes a clean-cut change, that is, the boundary of the thick disk is observed (Fig.8b). Transition from the thick disk to the halo occurs at small values of stellar number density. The boundary of the halo ($Z = 8$ kpc) can be estimated approximately because of lack of data, but the existence of a halo is of no doubt. Thus, the galaxy

NGC 4244 has a thick disk 5.4 kpc in thickness and a halo with low surface density, having a thickness of 16 kpc.

6 Observational model of stellar structure of a spiral galaxy

On the basis of earlier studies of the stellar population of three spiral galaxies, we present a model of stellar structure of a spiral galaxy [15]. We considered in this model the variation of the number density of different-type stars along the radius of the galaxy from bulge to halo. It was shown that the boundaries of the thin disk are well defined by the region of distribution of young stars. The boundary of the thick disk and halo are defined by the bend point of the number density gradient of old stars – red giants. However, due to the lack of data, we failed to present the distribution of different type stars perpendicular to the galactic plane. But it is exactly such distribution give an conception of the three – dimensional shape of galaxies. In the present paper we took as a basis this, the already mentioned model, but added to it our new results on the investigation of the distribution of stars in the galaxies along the Z axis (Fig.9).

Qualitatively, the distribution of stars both along the radius of the galaxy and along the Z axis are alike. Young stars occupy the region of the thin disk, intermediate age stars form a structure of a larger size, while old stars form the thick disk and halo. The results of stellar structure of three massive irregular galaxies, IC 10, M 82, NGC 3077, where we have found the existence of thick disks and halos fall within this model. A similar at the first sight, model of composition of spiral galaxies, one can find in any book. The differences are in that the models of stellar structure of spiral galaxies presented earlier are constructed to a considerable degree on the basis of the spatial structure of the only Galaxy or on speculative assumption without references to particular investigations. Presenting results of investigation of the stellar structure of a great number of spiral galaxies, which are consistent with one another, we hope the observational data that we have obtained will facilitate creation of theoretical models of origin and evolution of spiral and irregular galaxies.

7 Discussion

Resolution of galaxies into stars will make it possible to investigate the spatial distribution of different types stars, both young and intermediate age star or old stars, in galaxies. The possibility of selection of stars by their types makes the method of counting stars basically different from the method of surface photometry since it provides a possibility of dividing stars of different luminosity and age but of similar colour (for instance, AGB and RGB stars). A second distinction of the method of counting stars is that it makes possible to reveal spatial stellar structures of very low surface brightness, which cannot be done by the method of surface photometry. We have used the indicated advantages to clear up the composition and extent of stellar structures of three edge-on spiral galaxies. Under investigations of these galaxies, NGC 891, NGC 4144 and NGC 4244, it was ascertained that although morphologically all of them have the same structure: a thin and thick disks and halo, but the relative dimensions of the thick disk and halo change within a wide range. Nor does the surface brightness of the halo remain constant at border with the thick disk. Whereas in NGC 891 the halo extends to the size $Z = 23$ kpc and has high surface brightness, in NGC 4244 the halo is three times as small and has a low surface brightness which turned out to be barrier to its detection by the method of surface photometry [36]. Taking into consideration the accidental choice of the galaxies and also the fact we already revealed earlier thick disks and halos in three spiral galaxies one may consider with high probability that the thick disks and halos composed from old stars are necessary components of spiral galaxies. Apart from the galaxies discussed in the present paper, the edge-on galaxies IC 2233, IC 5052 and NGC 4631 have a quite similar structure, which chances statistical significance of the results that we have obtained. It is natural that the process of interaction of galaxies can distort the stellar structure, and our conclusions are inapplicable to such galaxies.

8 Conclusions

Based on the method of number density calculation of stars, an investigation of stellar structures of three spiral galaxies viewed edge-on has been carried out. The study of the stellar population of different age has made it possible to obtain the following results:

- a) For the first time, thick disks and halos constituted mainly from red giants have been revealed in the galaxies NGC 891, NGC 4144 and NGC 4244.
- b) The difference between the stellar density gradients of the thick disk and halo, which we found earlier, has been confirmed, which allows their spatial sizes to be objectively determined.
- c) It has been established that halos of spiral galaxies have a shape oblate at the galaxy poles, which is likely to point to its rotation
- d) Based on the photometry of red giants the distances of the galaxies NGC 891 and NGC 4144 have been measured for the first time.
- e) On the basis of the results obtained a model of stellar structure of spiral galaxies is presented. The use of the method of counting of stars has shown that measurements of stellar number density can be successfully employed for revealing of stellar subsystems and establishment of boundaries between thick disks and halos.

This work was done under the support of RFBR grant 03-02-16344.

References

1. Vallenari A., Bertelli G., Schmidtobreick L., *Astron. Astrophys.*, 361, 73, 2000.
2. Prochaska J.X., Naumov S.O., Carney B. W., McWilliam A., Wolfe A. M., *Astron. J.*, 120, 2513, 2000.
3. Chiba M., Beers T.C., *Astron. J.*, 119, 2843, 2000.
4. Zoccali M., Renzini A., Ortolani S., Greggio L., Saviane I., Cassisi S., Rejkuba M., Barbuy B., Rich R.M., Bica E., astro-ph/0210660, 2002.
5. Williams B.F., *Mon. Notic. Roy. Astron. Soc.*, 331, 293, 2002.
6. Rowe J.F., Richer H.B., Brewer J.P., Grabtree D.R., astro-ph/0411095, 2004.
7. Schombert J.M., Bothum G.D., *Astron. J.*, 93, 60, 1987.
8. Dalcanton J.J., Bernstein R.A., *Astron. J.*, 124, 1328, 2002.
9. Minniti D., Zijlstra A. A., *Astrophys. J.*, 467, 13, 1996.
10. Minniti D., Zijlstra A. A., Alonso M. V., *AJ*, 117, 881, 1999.
11. Tikhonov N.A., Dissertation, St.-Peterburg, Russia, 2002.
12. Tikhonov N.A., accepted to *Astronomy Reports*, 2005a.
13. Tikhonov N.A., submitted to *Astronomy Reports*, 2005b.
14. Drozdovsky I., Tikhonov N., Schulte-Ladbeck R., "The outer stellar edges of irregular galaxies: IC10 and LeoA", *STScI May*, 2003.

15. Tikhonov N.A., Galazutdinova O.A., Drozdovsky I., *Astron. Astropys.*, 431, 127, 2005.
16. Gonzalez J.J., PhD thesis Univ. California, Santa Cruz, 1993.
17. Cantiello M., Raimondo G., Brocato E., Capaccioli M., *Astron. J.*, 125, 2783, 2003.
18. Pasquini L., Bonifacio P., Randich S., Galli D., Gratton R.G., *astro-ph/0407524*, 2004.
19. Howk J.C., Savage B.D., *Astron. J.*, 114, 2463, 1997.
20. van der Kruit P., Searle L., *Astron. Astropys.*, 95, 116, 1981.
21. Garcia-Burillo S., Guelein M., Cernicharo J.J., Dahlem M., *Astron. Astropys.*, 266, 21, 1992.
22. Swaters R.A., Sancisi R. and van der Hulst J.M., *Astrophys. J.*, 491, 140, 1997.
23. Fraternali F., Oosterloo T., Recycling intergalactic and interstellar matter IAU Symposium Series, v. 217, *astro-ph/0310799*, 2004.
24. Fraternali F., Oosterloo T., Sancisi R., Swaters R., *astro-ph/0410375*, 2004.
25. Martin M.C., *Astron. Astrophys. Suppl. Ser.*, 131, 77, 1998.
26. Xilouris E. M., Alton P. B., Davies J. I., Kylafis N. D., Papamastorakis J., Trewhella M., *Astron. Astrophys.*, 331, 894, 1998.
27. Spitzer L., *Physical Processes in the Interstellar Medium*, New York, Wiley-Interscience, (p.162), 1978.
28. Hunter D.A., Gallagher J.S. III, *Astron. J.*, 90, 1789, 1985.
29. Alonso-Herrero A., Knapen J.H., *Astron. J.*, 122, 1350, 2001.
30. Garcia-Ruiz I., Sancisi R., Kuijken K., *Astron. Astrophys.*, 394, 769, 2002.
31. Swaters R. A., van Albada T. S., van der Hulst J. M., Sancisi, R., *Astron. Astropys.*, 390, 829, 2002a.
32. Swaters R. A., Balcells M., *Astron. Astrophys.*, 390, 863, 2002b.
33. Hummel E., Sancisi R., Ekers R. D., *Astron. Astrophys.*, 133, 1, 1984.
34. Olling R.P., *Astron. J.*, 112, 457, 1996.
35. Kodaira K., Yamashita T., *Publ. Astr. Soc. Jap.*, 48, 581, 1996.
36. Fry A.M., Morrison H.L., Harding P., Boroson T. A., *Astron. J.*, 118, 1209, 1999.
37. Stetson P.B., *Users Manual for DAOPHOT II*, 1994. 38. Dolphin A.E., *Publ. Astr. Soc. Pacif*, 112, 1383, 2000.

39. Holtzmann J.A., Hester J.J., Casertano S., Publ. Astr. Soc. Pacif., 107, 156, 1995a.
40. Holtzmann J.A., Burrows C.J., Casertano S., Hester J.J., Trauger J.T., Watson A.M., Worthey G., Publ. Astr. Soc. Pacif., 107, 1065, 1995b.
41. Lee M.G., Freedman W.L., Madore B.F., Astrophys. J., 417, 553, 1993.
42. Ferrarese L., Mould J.R., Kennicutt R.C et al., Astrophys. J, 529, 745, 2000.
43. Karachentsev I.D., Drozdovsky I.O., Astron. Astrophys. Suppl. Ser., 131, 1, 1998.
44. Karachentsev I.D., Sharina M.E., Dolphin A.E., Grebel E.K., Geisler D., Guhathakurta P., Hodge P.W., Karachentseva V.E., Sarajedini A., Seitzer P., Astron. Astrophys., 398, 467, 2003.
45. de Grijs R., van der Kruit P.C., Astron. Astrophys. Suppl. Ser., 117, 19, 1996.
46. Zucker D., Kniazev A., Bell E., Martinez-Delgado D., Grebel E., Rix H,W., Rockosi C., Holzman J., Walterbos R. et al., Astrophys. J., 612, L117, 2004.
47. Schlegel D. J., Finkbeiner D.P., Davis M., Astrophys. J., 500, 525, 1998.

Table 1: Galaxies Data

Name	V_r	$a' \times b'$	B_t^0	Classification	A_b	A_v	A_i	i	$M - m$	M_{abs}
NGC 891	528	13.5×2.5	9.37	SA(s)b sp HII	0.280	0.215	0.126	90	29.96	-20.59
NGC4144	265	6.0×1.3	11.10	SAB(s)cd sp HII	0.065	0.050	0.290	84	29.30	-18.20
NGC4244	244	19.4×2.1	9.28	SA(s)cd:sp HII	0.090	0.069	0.040	90	28.16	-18.88

The Galactic extinction correction is by Schlegel et al.(1998).

The inclination is taken from LEDA.

Values of the $(M - m)$ and M_{abs} have obtained in this paper.

Table 2: Observational log of HST.

Galaxy	Region	Date	Band	R	Exposure	ID	N_{stars}
NGC891	S1	2003-02-19	F814w	2.12	2×2620+2472	9414	108970
		2003-02-19	F606w	2.12	2×2620+2472	9414	
	S2	2003-02-20	F814w	7.94	2×1000	9676	900
		2003-02-20	F606w	7.94	2×400+4×500	9676	
NGC4144	S1	2003-12-08	F814w	0.98	350	9765	63605
		2003-12-08	F606w	0.98	338	9765	
NGC4244	S1	2001-06-11	F814w	3.77	600	8601	9680
		2001-06-11	F606w	3.77	600	8601	
	S2	2001-06-30	F814w	2.09	6×500	9086	3945
		2001-06-30	F606w	2.09	6×500	9086	
	S3	2003-11-12	F814w	0.33	350	9765	115990
		2003-11-12	F606w	0.33	338	9765	

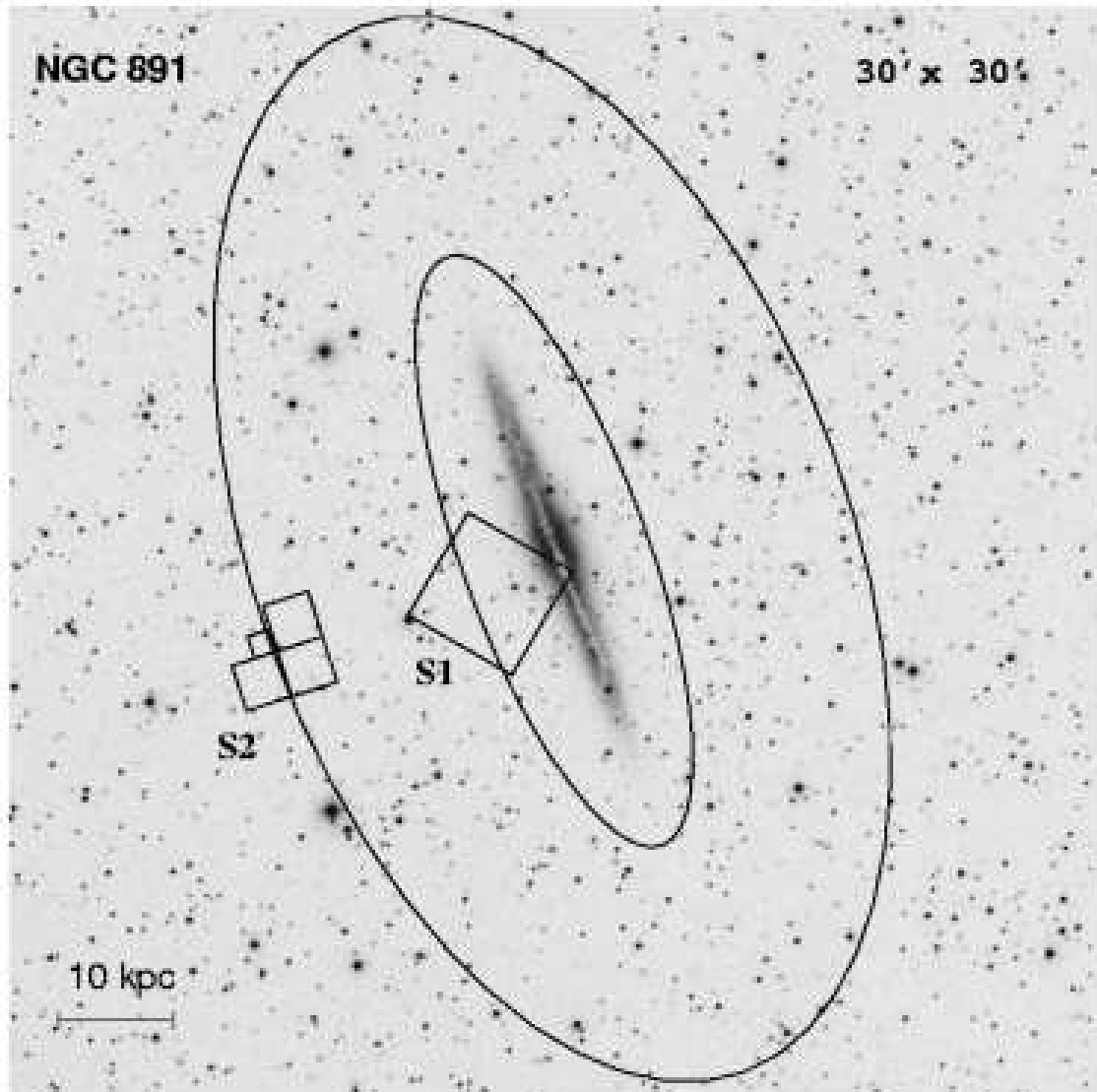


Figure 1: DSS-2 image of the galaxy NGC 891 with the S1 (ACS/WFC) and S2 (WFPC2) footprint overlaid. The inner ellipse shows the boundary of the thick disk, the outer one shows that of the halo.

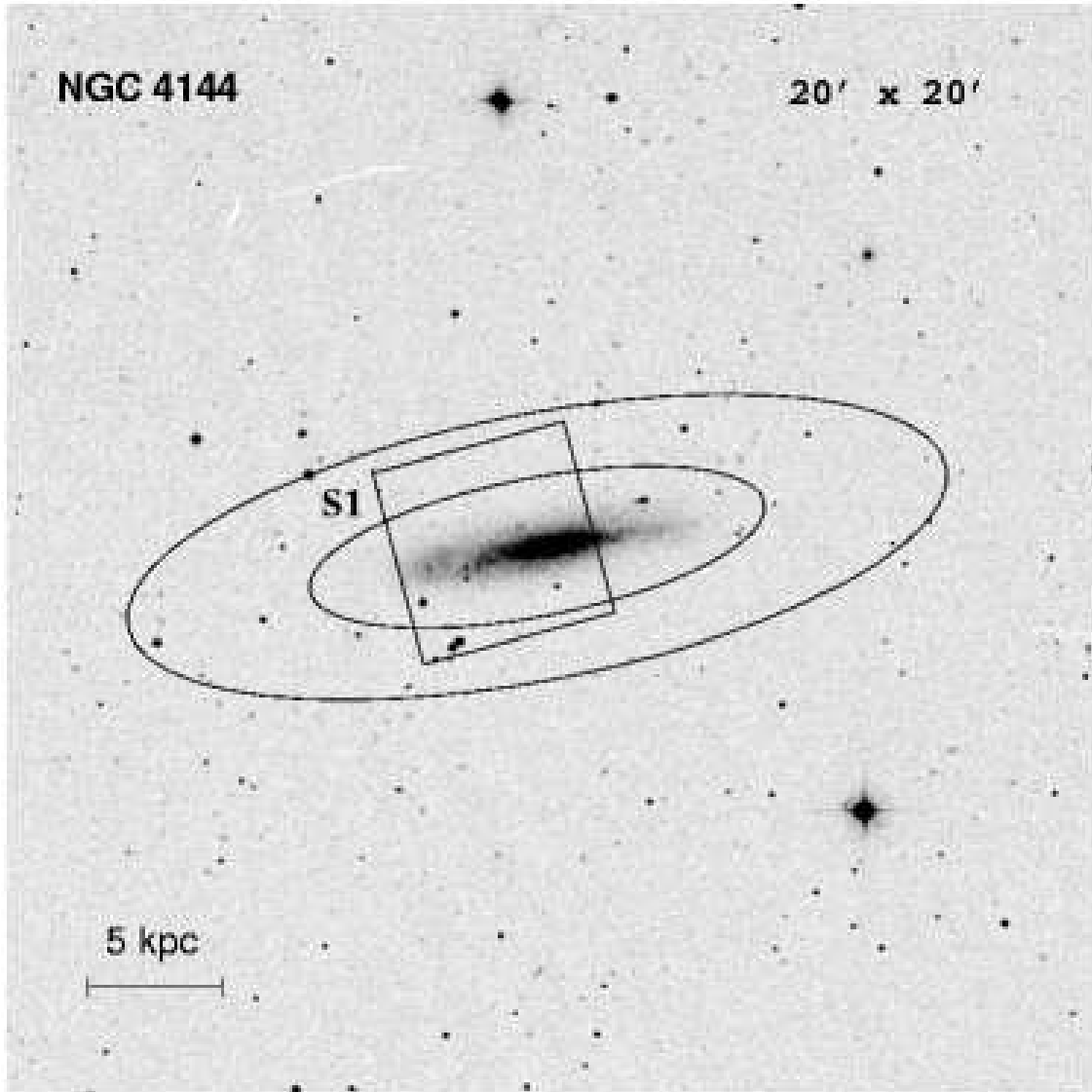


Figure 2: Same as in Fig.1 for the galaxy NGC 4144.

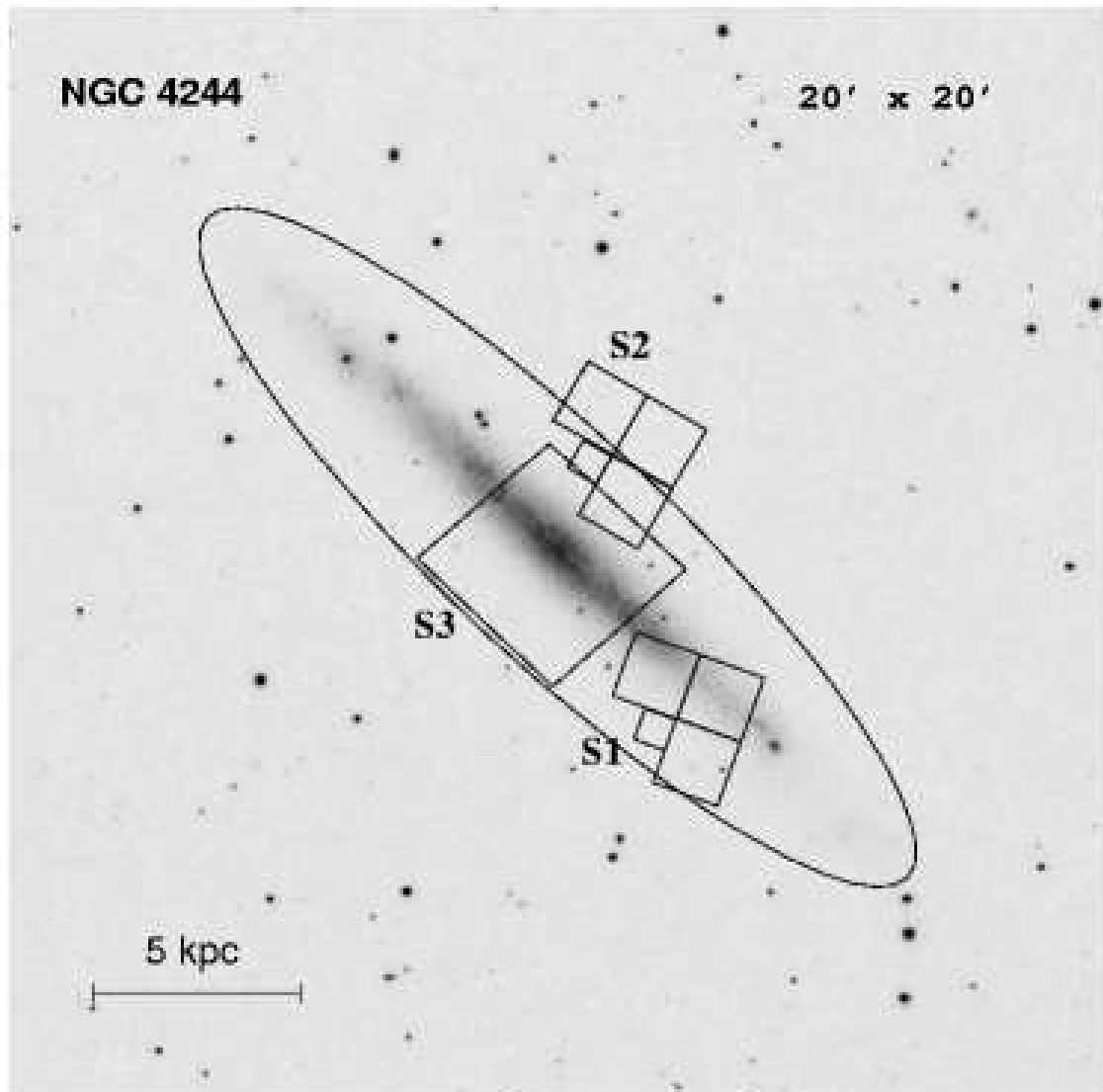


Figure 3: Same as in Fig1 for the galaxy NGC 4244. Only the boundary of the thick disk is marked.

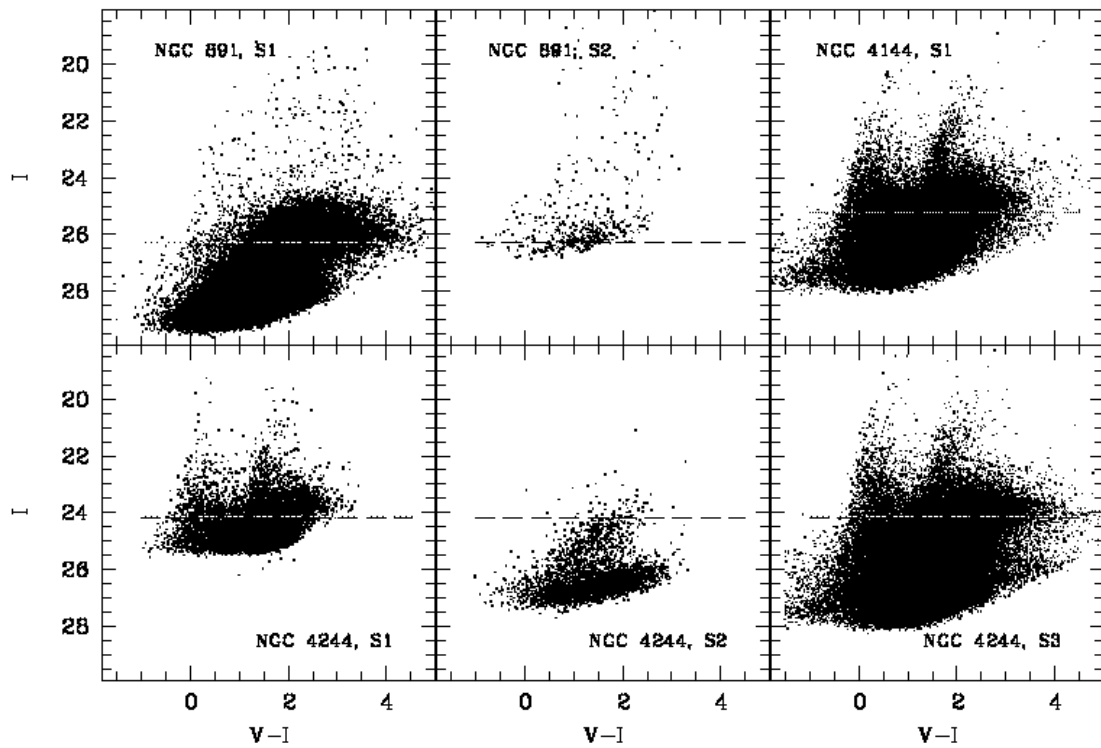


Figure 4: Color-Magnitude diagram for all fields of the studied galaxies. The dotted line marks the position of the tip of the red giant branch (TRGB).

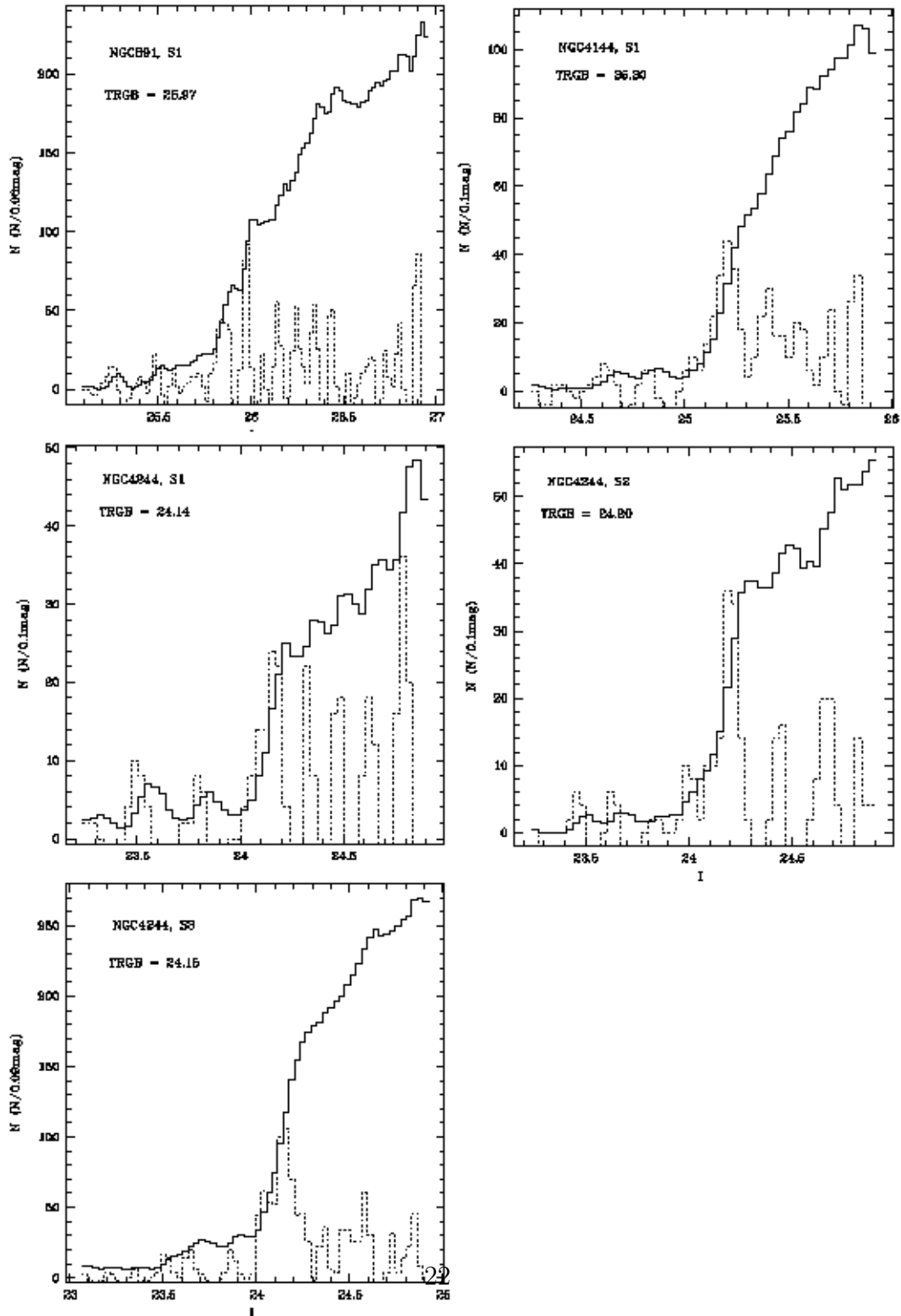


Figure 5: I band luminosity function of the stars in fields being investigated in. The sharp change in the number of stars corresponds to the beginning of the red giant branch, which is used to measure the distances (TRGB

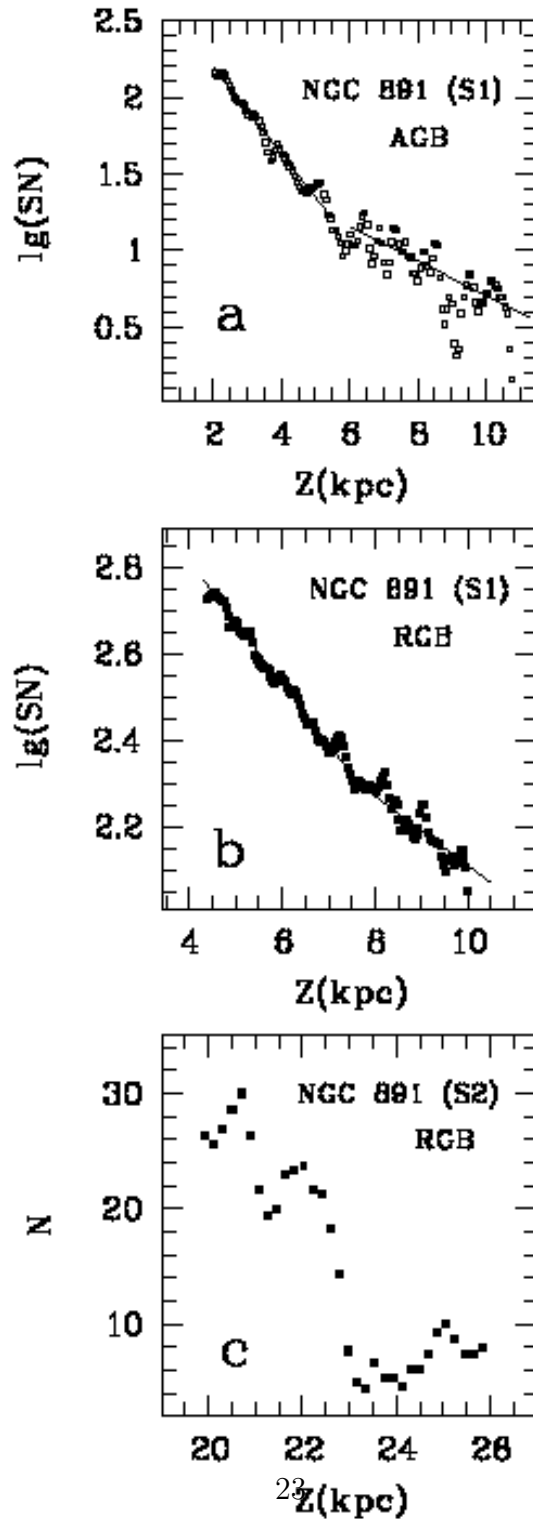


Figure 6: Number density distribution of AGB (a) and RGB (b) stars of NGC 891 at the border of the thick disk (field S1) and RGB stars (c) at the border of the halo (field S2). At $Z = 7.6$ kpc a bend of the number density of RGB stars corresponds to the transition from the thick disk to the halo.

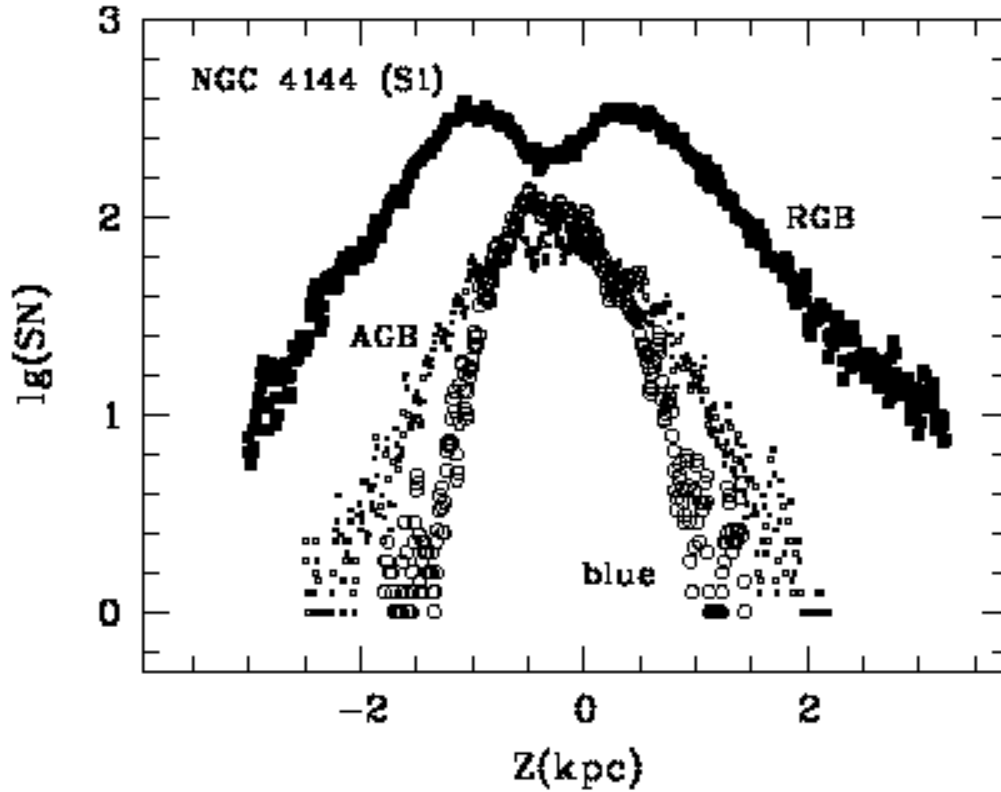


Figure 7: Distribution of the number of stars of different age perpendicular to the plane of galaxy NGC 4144. Open circles are young stars. Dots are the stars of intermediate age (AGB). Filled circles mark old stars (RGB). At $Z = 2.4$ kpc a change in the gradient of the number density of RGB stars corresponds to the transition from the thick disk to the halo.

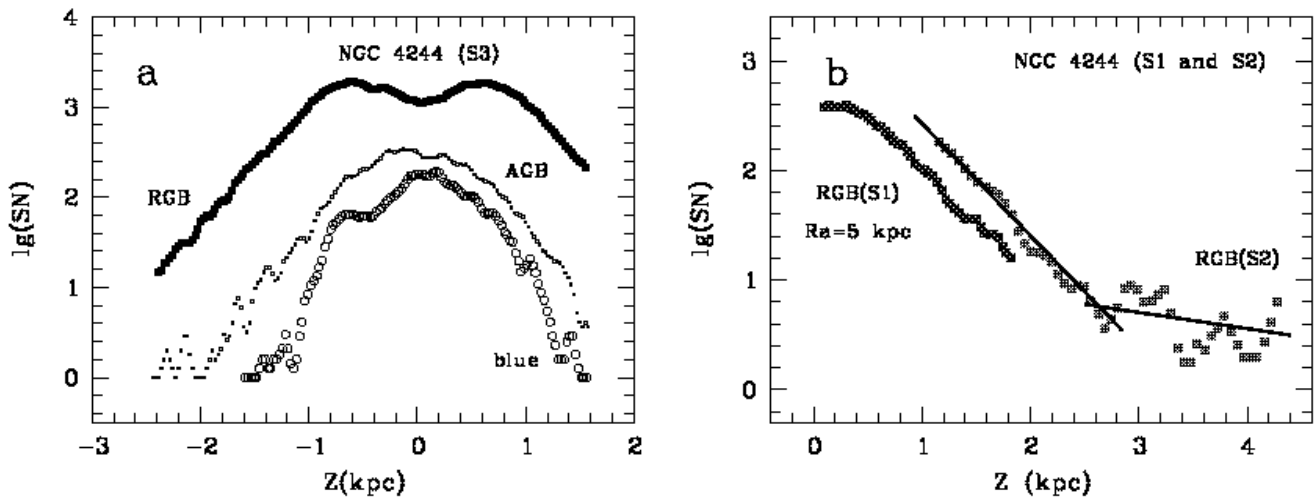


Figure 8: Same as in Fig.7 for the galaxy NGC 4244. It can be seen that the boundary of the thick disk is outside the field S3 (b). The distribution of old (RGB) stars in the fields S1 and S2 is perpendicular to the galaxy plane. At $Z = 2.7$ kpc transition from the thick disk to the halo is seen.

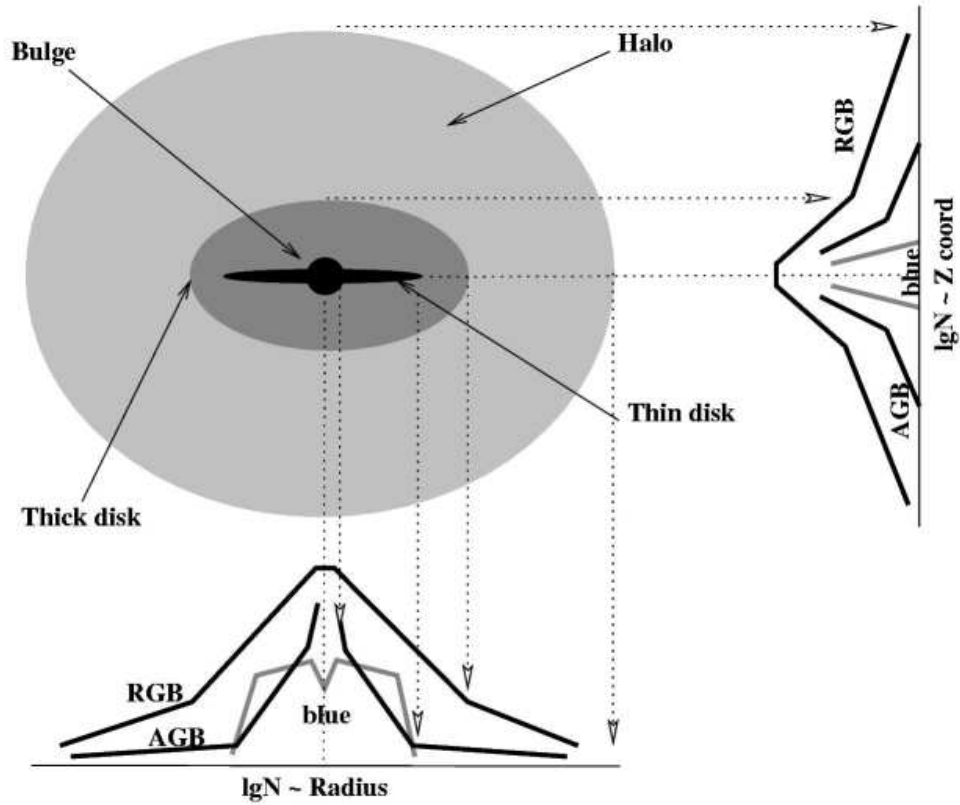


Figure 9: Three-dimensional model of the number density distribution of the stellar population along the radius and Z axis in spiral galaxies. Number densities of different type stars are given in relative units. The absolute sizes of the halo along the Z coordinate change from 8 to 25 kpc in each individual galaxy.